JOURNAL OF MATERIALS SCIENCE **34** (1999) 5649–5659

Influence of non-stoichiometric ordering on the electrostriction coefficient of lead magnesium niobate lead titanate compositions close to the morphotropic phase boundary

S. M. GUPTA, D. VIEHLAND
Department of Materials Science and Engineering, University of Illinois Urbana, IL 61801
E-mail: s.gupta@cranfield.ac.uk

The effect of non-stoichiometric ordering on the electrostriction of $Pb(Mg_{1/3}Nb_{2/3})O_3$-$PbTiO_3$ (PMN-PT) compositions (65/35) close to morphotropic phase boundary (MPB) has been studied using electrically induced strain and polarization methods. La was substituted (1 to 10 at %) on the A-site to control the degree of B-site cation ordering. The charge imbalance due to La^{3+} was compensated by two different mechanisms: (1) creation of B-site vacancies, and (2) changing the B-site cation ratio. Electrostriction coefficient measurements revealed dependencies on the degree of non-stoichiometric ordering and the charge compensation mechanism. A high value of the electrostriction coefficient was found to be accompanied by larger electrically-induced strains and smaller polarizations. In addition, the temperature dependence of the electrostriction coefficient was studied.

1. Introduction

Recently, interest in electrostrictive materials has increased because of their possible use as micropositioners in precise engineering applications [1–4]. Piezoelectric actuators are being replaced by electrostrictive actuators because the later have low hysteretic losses under ac electric field reversal, high displacements and displacement resolution, no need of poling, very fast response times, and small thermal expansion coefficients [5]. Lead magnesium niobate (PMN) has a large electrostriction effect near the temperature of its dielectric maxima [6–8]. In addition, the transition temperature can be shifted to room temperature by alloying with lead titanate (PT). Lead titanate forms a complete solid solution with PMN. A morphotropic phase boundary (MPB) exists near 32 at % PT [9].

Structural studies of PMN as a function of PT content have previously been reported by Viehland *et al.* [10]. This study demonstrated the presence of polar nanodomains for PT contents less than 30 at %, tweedlike structure for PT contents between 30 and 35 at %, and normal micron-sized ferroelectric domains for PT contents greater than 35 at %. In addition, La-modification of PMN-PT was found to result in the evolution of polar nanodomains and relaxor characteristics from the tweedlike structures. Other studies by Chen *et al.* [11] and Randall *et al*. [12] have reported the presence of short-range ordered domains on the scale of 2 to 5 nm which were characterized by the presence of 1/2 [111] superlattice reflections. These ordered regions did not coarsen on heat treatment [13]. Furthermore, Chen *et al.* [11] suggested that the short range ordered regions in PMN had a local Mg/Nb ratio of 1 : 1, relative to the global ratio of 1 : 2. It was then proposed that this local charge imbalance resulted in the stabilization of short-range ordered domains. Evidence in support of this hypothesis was demonstrated by donor and acceptor modifications onto the A-site of PMN. It was concluded that the degree of ordering and the size of ordered domains can be enhanced and reduced by donor and acceptor modifications, respectively.

Electrostriction gives rise to a strain proportional to the square of the induced polarization. Electrostriction in PMN and PMN-10PT has previously been extensively studied [14, 15] for possible use as actuators. The purpose of the present work was to study the effect of non-stoichiometric ordering on the electrostriction coefficient of PMN-PT solid solutions near the MPB. La-modification (1 to 10 at %) was used to enhance the degree of B-site cation ordering. Two different charge compensation mechanisms were studied: (1) creation of B-site vacancies while maintaining the B-site cation ratio constant, and (2) changing B-site cation ratio. The influence of the charge compensation mechanisms and the degree of B-site cation ordering on the electrically induced strain and polarization, and the electrostriction coefficient were determined.

2. Experimental

The specimens studied in this investigation were fabricated according to the formula:

(a) $Pb_{1-x}La_x[(Mg_{1/3}Nb_{2/3})_{0.65}Ti_{0.35}]_{1-x/4}O_3$ (La-PMN-PT B-x/65/35) for $0 < x < 0.1$, where La^{3+} is compensated by creating B-site vacancies, and

(b) $Pb_{1-x}La_x[(Mg_{1+x/3}Nb_{2-x/3})_{0.65}Ti_{(1-x/4)0.35}]O_3$ (PLMN-PT C-x/65/35) for $0 < x < 0.1$, where La^{3+} is compensated by changing Mg/Nb/Ti ratio on the B-site.

The purity and processing details have been presented in a previous publication [16]. The calcined and sintered specimens were analyzed by X-ray diffraction (XRD) (Rigaku, D-max CuK_α radiation) for second phase formation. The density of the sintered samples was found to be above 95% of the theoretical. The sintered blocks were cut into thin disks and polished

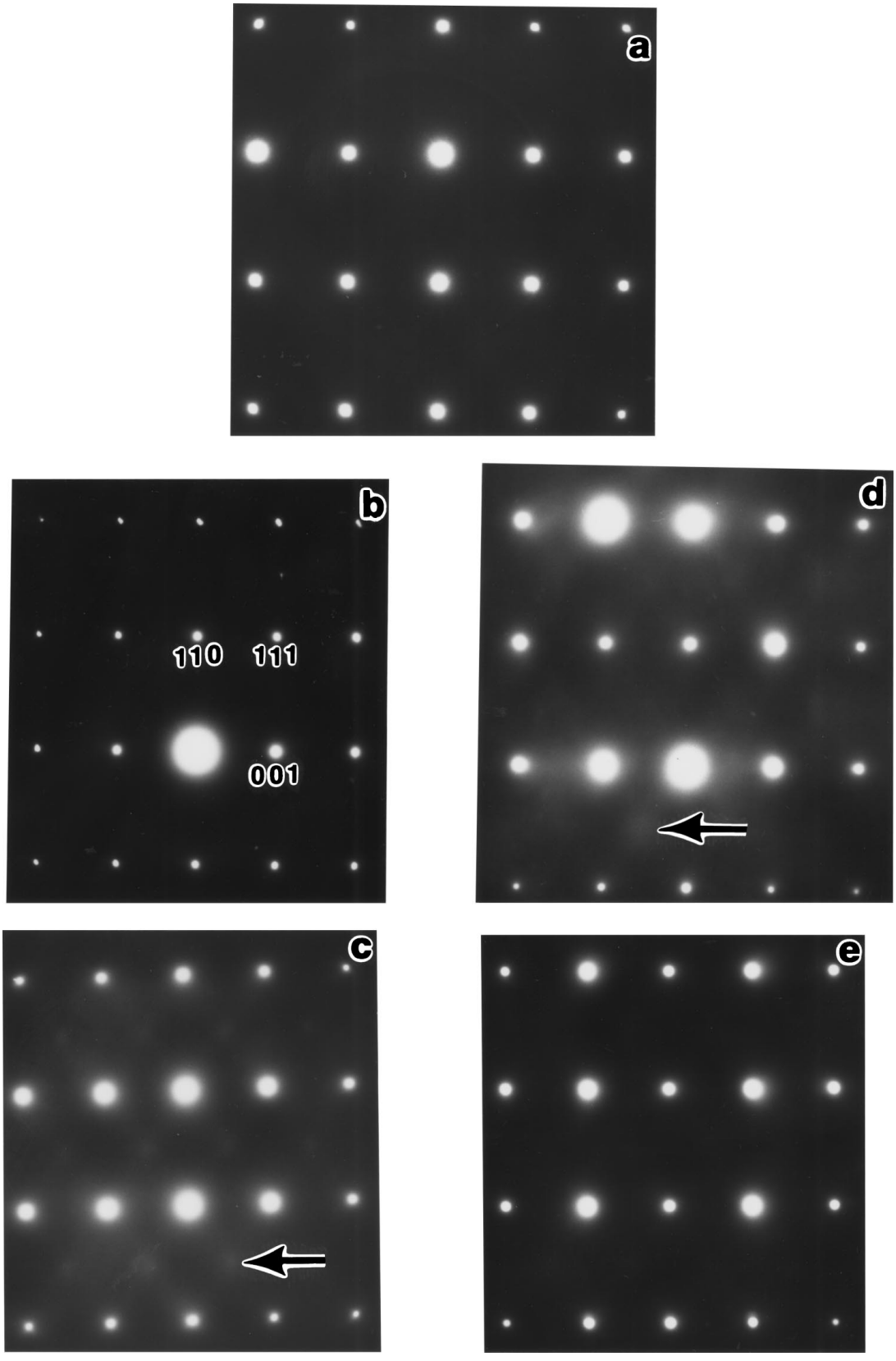

Figure 1 Selected area electron diffraction along ⟨110⟩ unit axis for various La/PMN/PT compositions: (a) 0/65/35, (b) B-5/65/35, (c) B-10/65/35, (d) C-5/65/35 and (e) C-10/65/35.

on different grades of emery paper to obtain parallel surfaces. The polished surfaces were ultrasonically cleaned to remove dust particles and then annealed at 650 °C for half an hour to remove surface strains during polishing. Electroding was carried out by sputtering gold, followed by a thin coating of air dried silver paint.

The dielectric response was measured using a Hewlett-Packard 4284A inductance-capacitance-resistance (LCR) bridge which can cover a frequency range from 20 to 10^6 Hz. For low temperature measurements, the samples were placed in a Delta Design 9023 test chamber, which could be operated between −180 and +250 °C. The temperature was measured using a HP 34401A multimeter, via a platinum resistance thermocouple mounted directly on the ground electrode of the sample fixture. Measurements were performed on cooling and heating, using a rate of 4 °C/min at frequencies 10^2, 10^3, 10^4, and 10^5 Hz.

Field induced longitudinal strain measurements were made using a linear variable differential transformer (LVDT) at 1 Hz frequency. Electrically-induced polarization studies were performed using a modified Sawer-Tower technique. For high temperature measurements, the sample holder was immersed in silicon oils (100

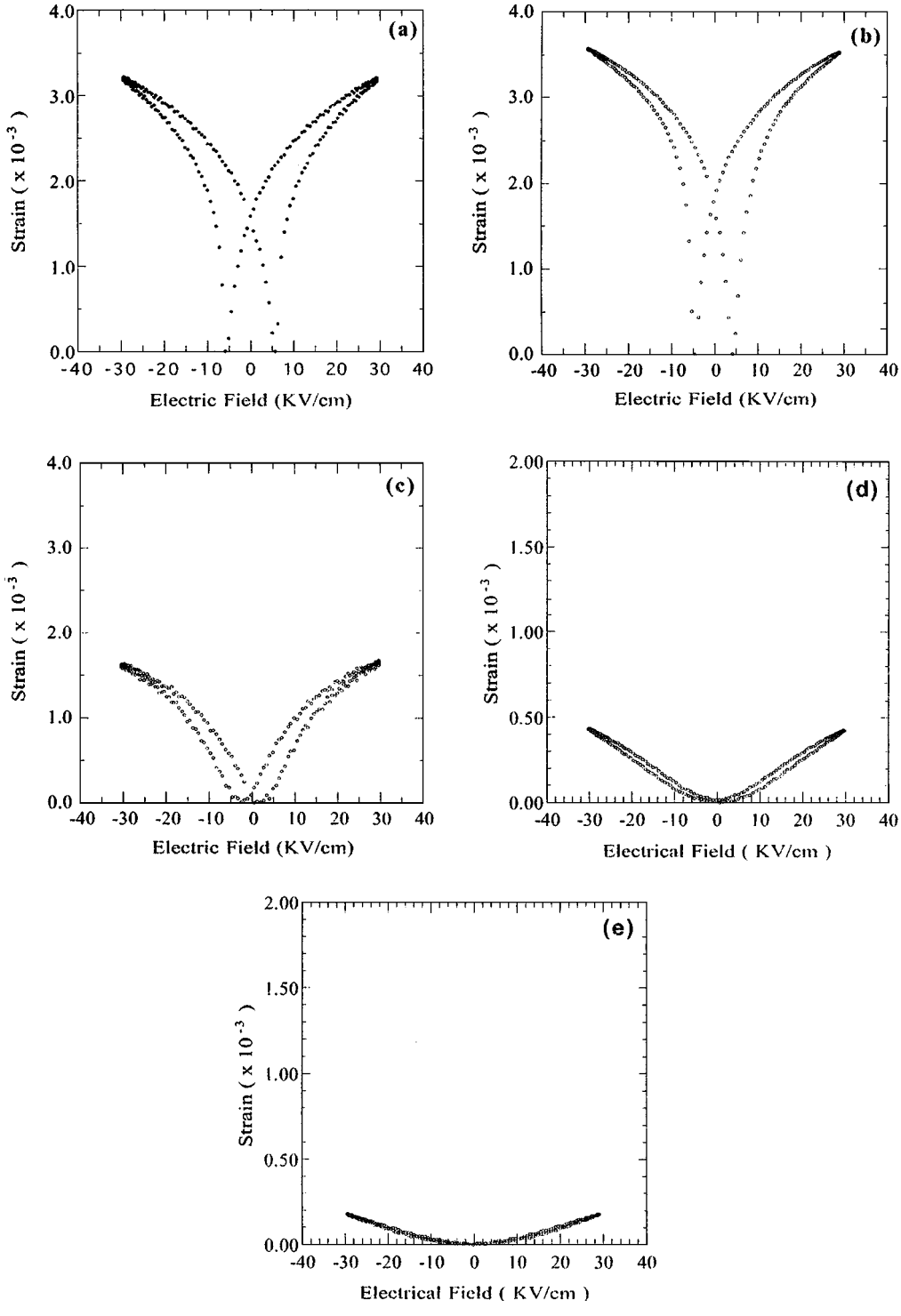

Figure 2 Electrically induced strain for various B-*x*/65/35 compositions: (a) 0/65/35, (b) B-2/65/35, (c) B-5/65/35, (d) B-8/65/35 and (e) B-10/65/35.

CS, Dow Corning) and heated in a oil bath circulator (Haake F3 circulator) between 25 to 200 °C.

Transmission electron microscopy (TEM) specimens were prepared by ultrasonically drilling 3-mm discs which were mechanically polished to ~100 μm. The center portions of these discs were then further ground by a dimpler to 10 μm, and argon ion-milled to perforation. Specimens were coated with carbon before examination. The TEM studies were done on a Phillips EM-400 microscope operating at an accelerating voltage of 120 kV.

3. Results and discussion

3.1. Selected area electron diffraction

Fig. 1a–e illustrate the ⟨110⟩ selected area electron diffraction (SAED) patterns for the compositions 0/65/35, B-5/65/35, B-10/65/35, C-5/65/35 and C-10/65/35, respectively. [Specimens in which La^{3+} was compensated by B-site vacancies and changing B-site cations ratio are represented by B-*x*/65/35 and C-*x*/65/35, respectively]. Superlattice reflections are clearly evident for B-10/65/35 and C-5/65/35 and are marked by an arrow in Fig. 1. However, only weak

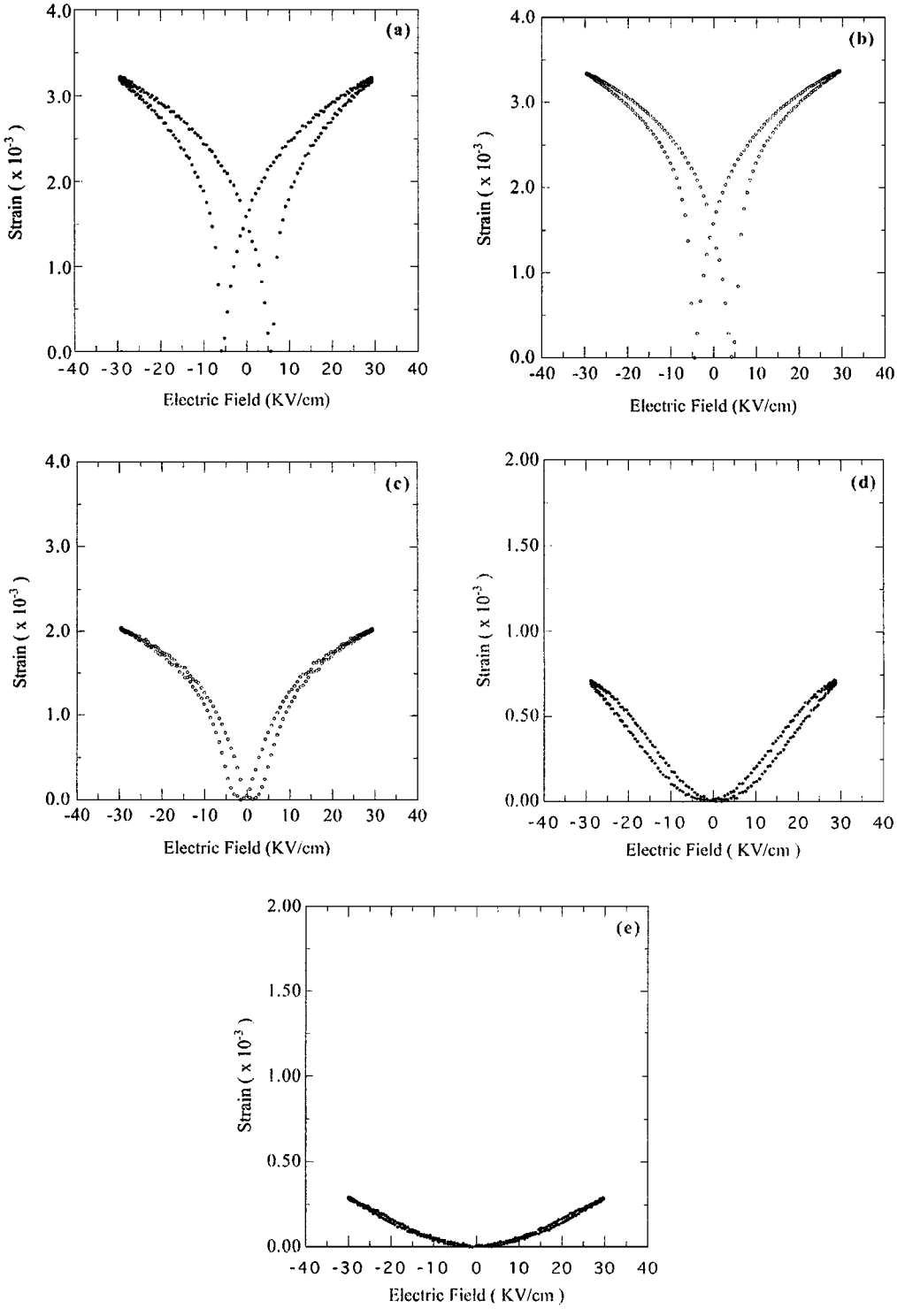

Figure 3 Electrically induced strain for various C-*x*/65/35 compositions: (a) 0/65/35, (b) C-2/65/35, (c) C-5/65/35, (d) C-8/65/35 and (e) C-10/65/35.

diffuse reflections were observed for C-10/65/35. In general, it was observed that the superlattice reflection intensity increased with increasing La-content between 0 and 10 at % for compositions in the B-*x*/65/35 sequence. Furthermore, the superlattice reflection intensity for C-10/65/35 was less than that for C-5/65/35. It has already been reported [16] that pyrochlore formation occurs when La^{3+} was compensated by creating B-site vacancies. However, no second phase was observed when La^{3+} was compensated by changing the B-site cations ratio. The volume fraction of the pyrochlore second phase for the B-*x*/65/35 and C-*x*/65/35 compositional sequence are compared in Table I.

The trend of increasing 1/2 ⟨111⟩ superlattice reflection intensity for the B-*x*/65/35 compositional sequence with increasing La-content is consistent with a previous investigation by Chen *et al.* [11]. However, for C-*x*/65/35 compositional sequence only diffuse 1/2 ⟨111⟩ reflections were observed, rather pyrochlore formation was evident with increasing La-concentration. This formation of pyrochlore phase could potentially be stopped by a valency change of transition metal cations or by a redistribution of oxygen [17, 18]. However, in the known mixed B-site cation relaxors, all metal cations exist in their highest oxidation state and the oxygen framework remains immobile.

TABLE I Phase analysis comparison for B-*x*/65/35 and C-*x*/65/35 sequences

La-content	Pyrochlore phase (%) (B-*x*/65/35)	Pyrochlore phase (C-*x*/65/35)
0	0	—
2	0	0
5	6	0
8	9	0
10	14	2

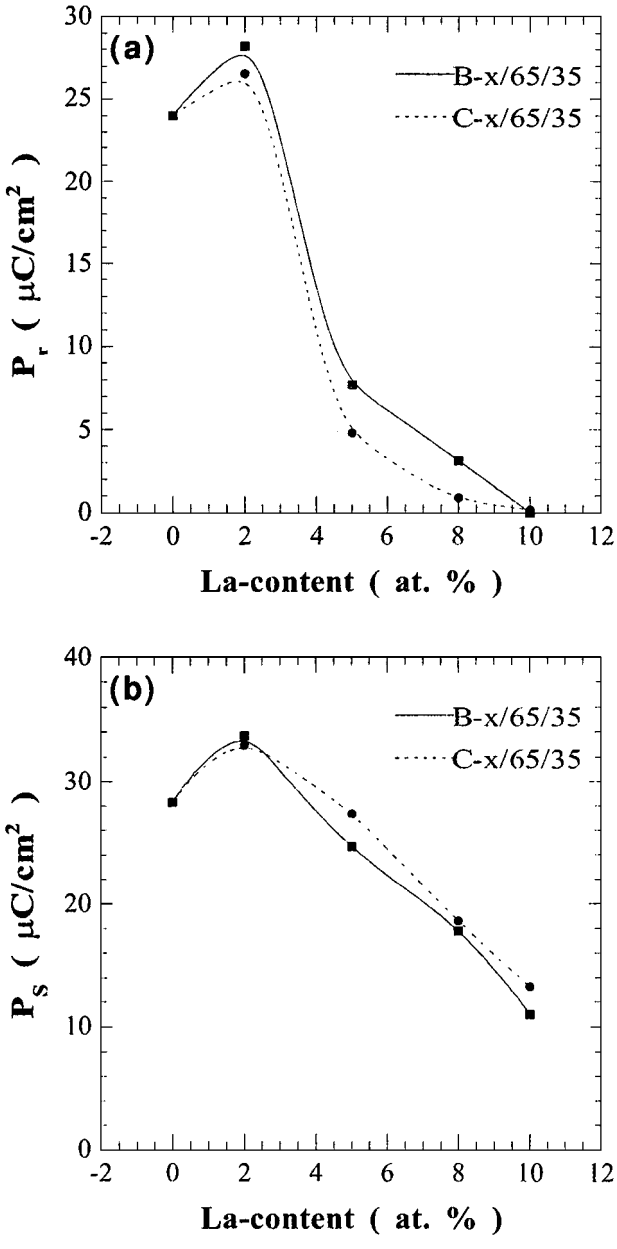

Figure 4 Comparison of (a) remanent polarization and (b) saturation polarization as a function of La-content for B-*x*/65/35 and C-*x*/65/35.

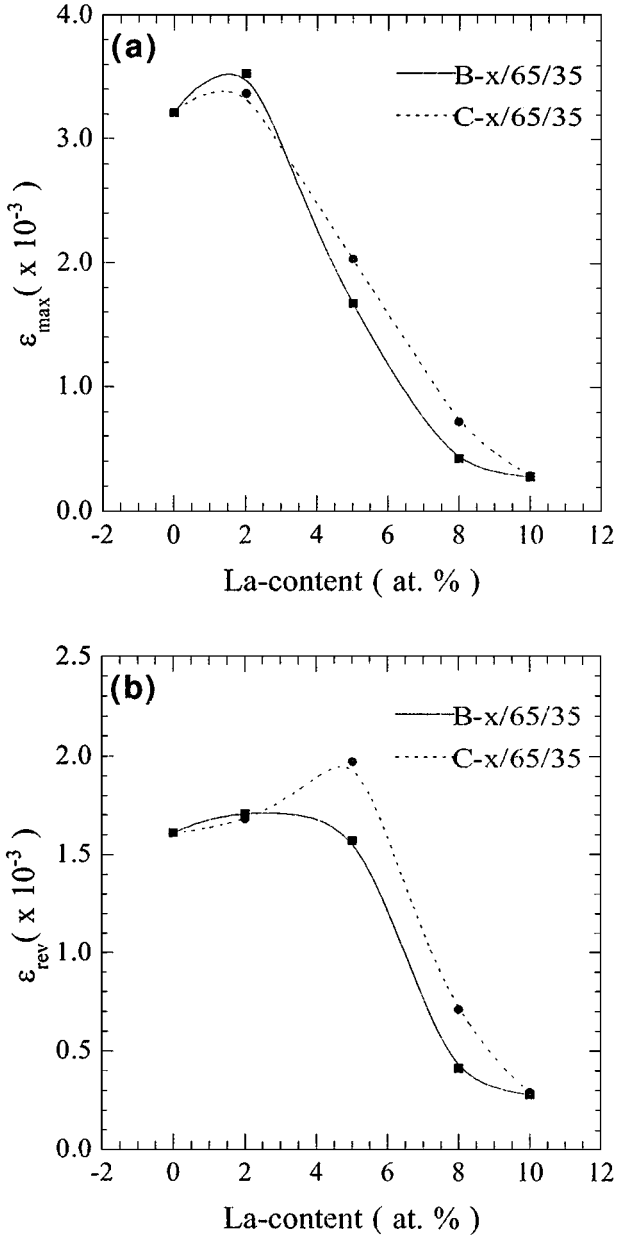

Figure 5 Comparison of (a) maximum electrically induced strain and (b) reversible electrically induced strain as a function of La-content for B-*x*/65/35 and C-*x*/65/35.

3.2. Electrically-induced polarizations and strains

Figs 2a–e and 3a–e show the electrically-induced strains for various compositions in the B-x/65/35 and C-x/65/35 sequences, respectively. A common ε-E behavior was observed for both sequences. At low La-substitutions (<5 at %), the shape of the ε-E loops were "butterfly like" typical of a piezostrictive coupling, and

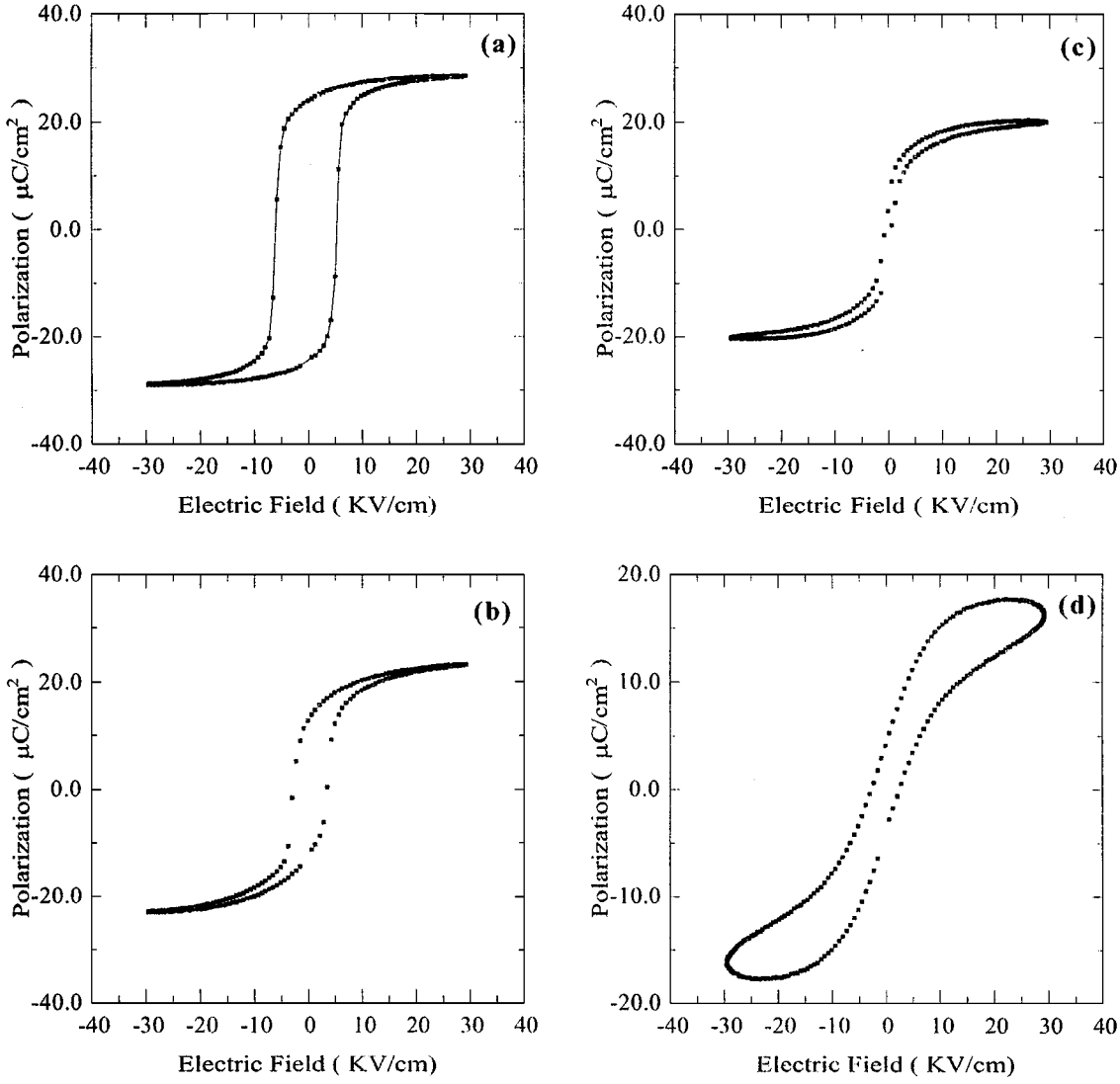

Figure 6 Temperature dependence of the polarization electric field (P-E) behavior of PMN/PT (65/35) at different temperatures: (a) 25 °C, (b) 125 °C, (c) 175 °C, (d) 200 °C.

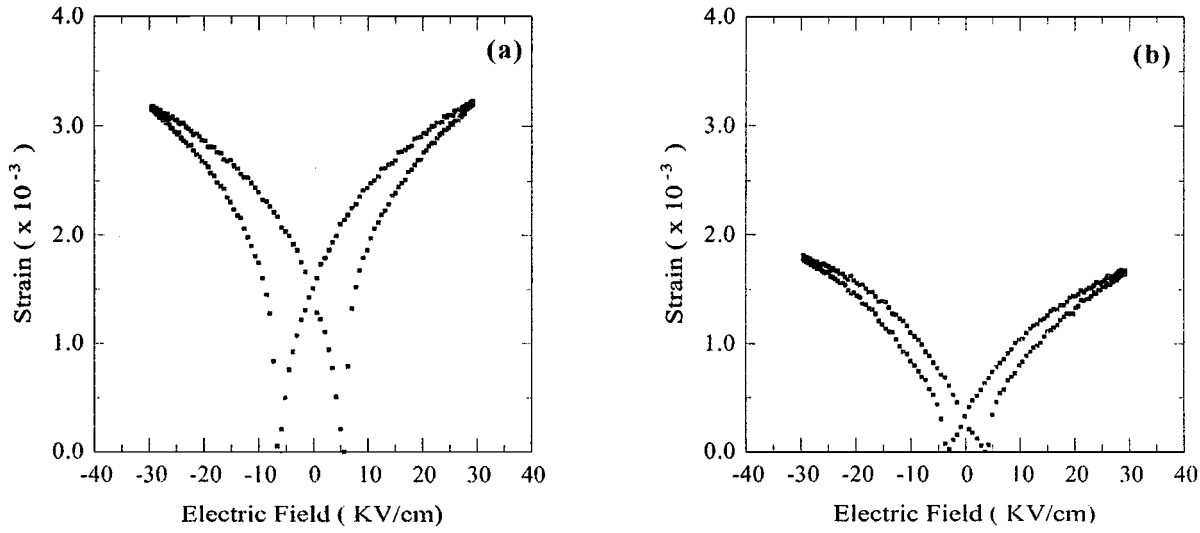

Figure 7 Temperature dependence of the electric field induced strain (ε-E) behavior of PMN/PT (65/35) at different temperatures: (a) 25 °C, (b) 125 °C, (c) 175 °C, (d) 200 °C. (*Continued*)

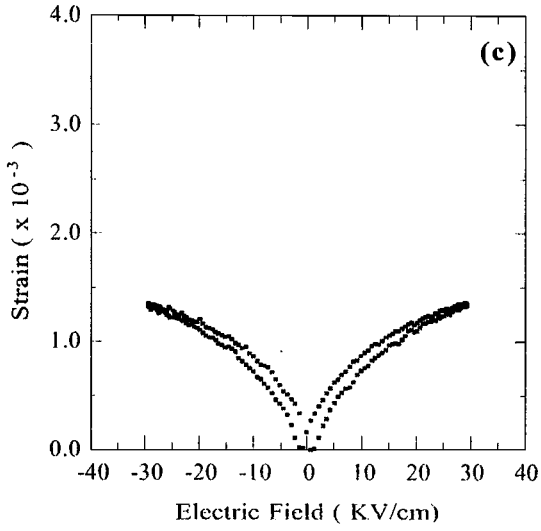

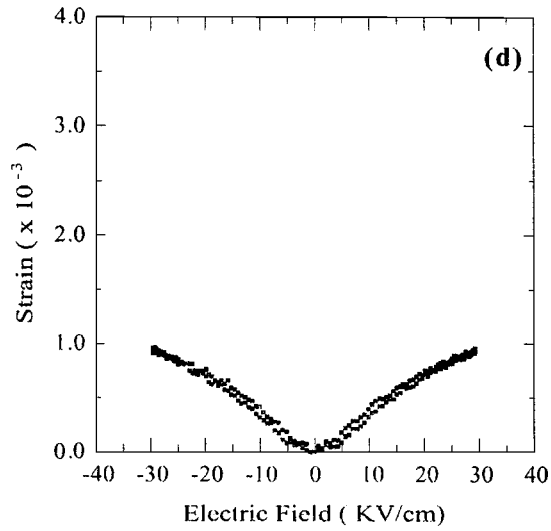

Figure 7 (*Continued*).

at high La-content (>5 at %) slim ε-E loop "quadratic like" typical of an electrostrictive coupling. The hysteretic losses was decreased considerably with increasing La-content for both sequences. Quadratic like behavior became evident near 5 at % La-content for both sequences. The major difference in these two sequences was the magnitude of the field induced strain (ε_{max}) accompanying the induced polarization. The remanent (P_r) and saturation (P_s) polarizations are compared for the B-x/65/35 and C-x/65/35 compositional sequences in Fig. 4a and b, respectively. It should be noticed that P_r drop more sharply with increasing La-content from 2 to 5 at % for the both compositional sequence. The remanent polarization value is higher and saturation polarization value is lower for B-x/65/35 than C-x/65/35 compositional sequences which is attributed to the non-stoichiometric ordering and pyrochlore phase.

To obtain a better understanding of the changes in the maximum induced strain under 30 kV/cm (ε_{max}) with La content, ε_{max} was broken down into two components, defined as the remanent strain (ε_{rem}) and the reversible strain (ε_{rev}), where $\varepsilon_{rem} + \varepsilon_{rev} = \varepsilon_{max}$. The change in ε_{max} and ε_{rev} with increasing La-content for the B-x/65/35 and C-x/65/35 compositional sequences are compared in Fig. 5a and b, respectively. On comparing these figures, it should be noticed that with increase La-content from 2 to 5 at % ε_{max} decreased more sharply for B-x/65/35 than for C-x/65/35. However, ε_{rev} exhibited a peak with increasing La-content between 2 and 5 at % for the C-x/65/35 compositional sequence, whereas a small increase in ε_{rev} was observed with increasing La-content below 5 at % for the B-x/65/35 compositional sequence.

The temperature dependence of the polarization and induced strain were then studied for the compositions 65/35, B&C-2/65/35 and B&C-5/65/35. Figs 6a–d and 7a–d show the induced polarization and strain at various temperatures for 0/65/35. Below ~180 °C a "butterfly like" ε-E loop, a strong hysteresis, and a remanent polarization were observed for 0/65/35. On heating, the ε-E curve changed to a "quadratic like" anhysteretic response, in addition only a small remanent polarization was sustained. A large hysteretic loss around 200 °C for 0/65/35 can be attributed to conductivity losses, which were also observed in tanδ measurements. It has

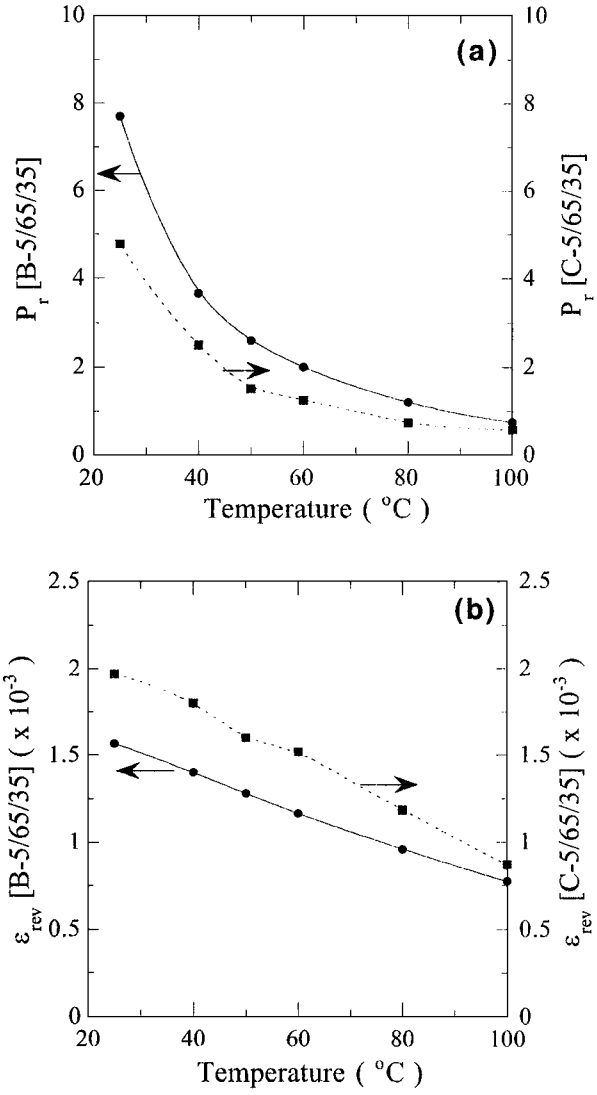

Figure 8 Comparison of (a) remanent polarization and (b) reversible strain as a function of temperatures for B-5/65/35 and C-5/65/35.

previously been reported [16] that 0/65/35 has normal micron-sized domains and a "butterfly like" ε-E response at room temperature, which changed to polar nanodomains and a quadratic like ε-E response by disrupting the ferroelectric coupling with increasing La-concentration. It seems that increasing temperature results in a similar decreased ferroelectric coupling and a "quadratic like" ε-E response.

The temperature dependence of P_r and ε_{max} for the compositions B-5/65/35 and C-5/65/35 are compared in Fig. 8a and b, respectively. It should be noticed that B-5/65/35 showed a larger P_r, than C-5/65/35 in the ferroelectric regions. A large value of P_r for B-5/65/35 can be explained using the "rigid-ion" model proposed by Uchino *et al.* [6] to explain "constant QC rule". Electron diffraction study revealed that non-stoichiometric ordering is stronger for C-5/65/35 than B-5/65/35. This means that B-5/65/35 is more disordered on the B-site positions than C-5/65/35. When an electric field is applied to the more disordered B-5/65/35, the B-site

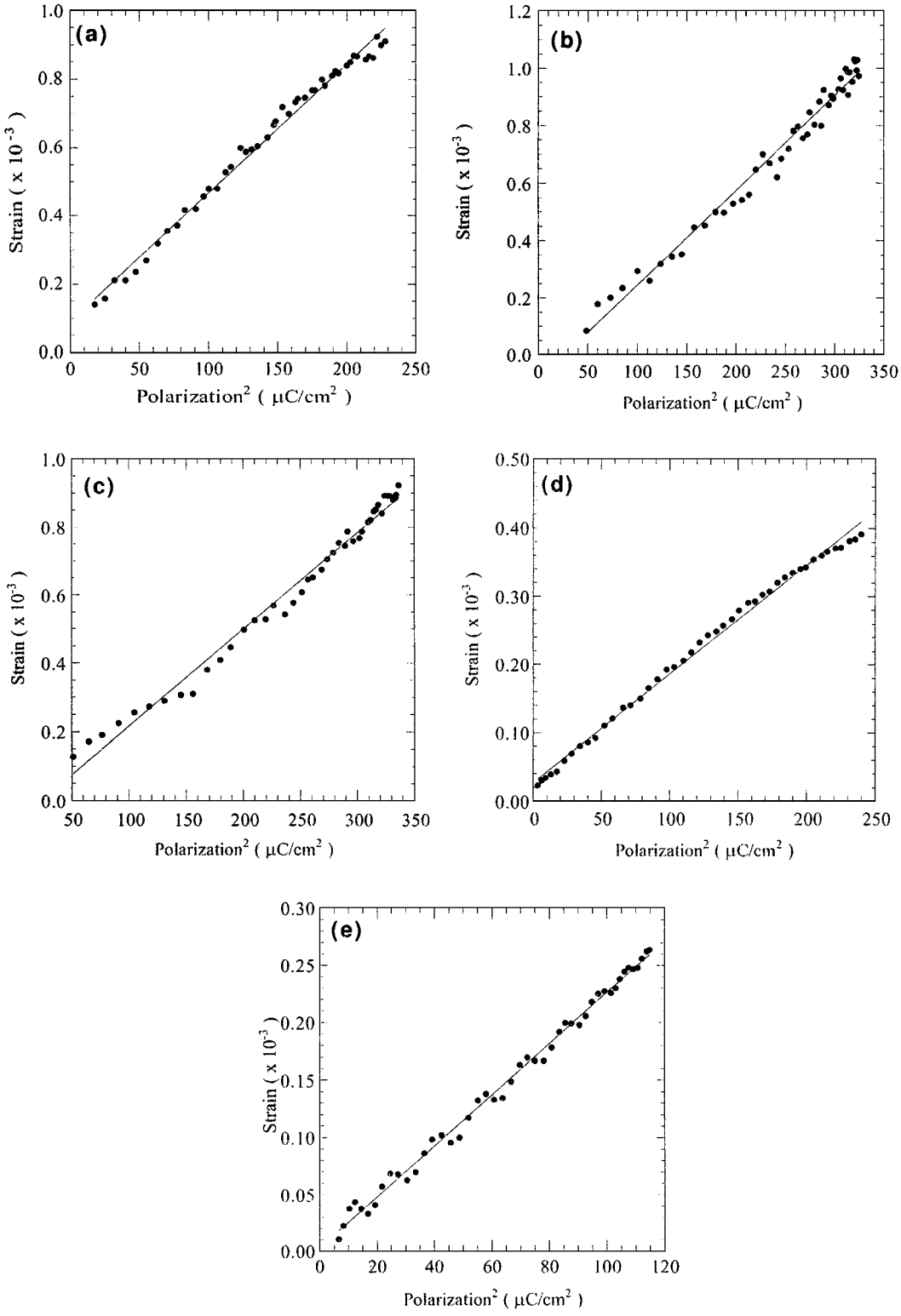

Figure 9 Electrically induced strain as a function of square of polarization in paraelectric region for (a) 0/65/35, (b) B-2/65/35, (c) B-5/65/35, (d) B-8/65/35 and (e) B-10/65/35.

cations can undergo larger displacements than in the more ordered C-5/65/35. Larger induced polarizations, smaller induced strains, and smaller Q_{11} values can be expected on applying an electric field for B-5/65/35, than for C-5/65/35. (In the following section, it will be confirmed that Q_{11} is smaller for B-5/65/35 than C-5/65/35). Furthermore, it should be noticed that B-5/65/35 and C-5/65/35 exhibited a sharper decrease in P_r near T_{max}. However, ε_{rev} was greater for C-5/65/35 than for B-5/65/35 in both the ferroelectric and paraelectric regions.

3.3. Electrostrictive coefficient

The electrically-induced strain is related to the electrostrictive coefficient, as given in Equation 1;

$$\varepsilon_{ij} = Q_{ijkl} P_k P_l \quad (1)$$

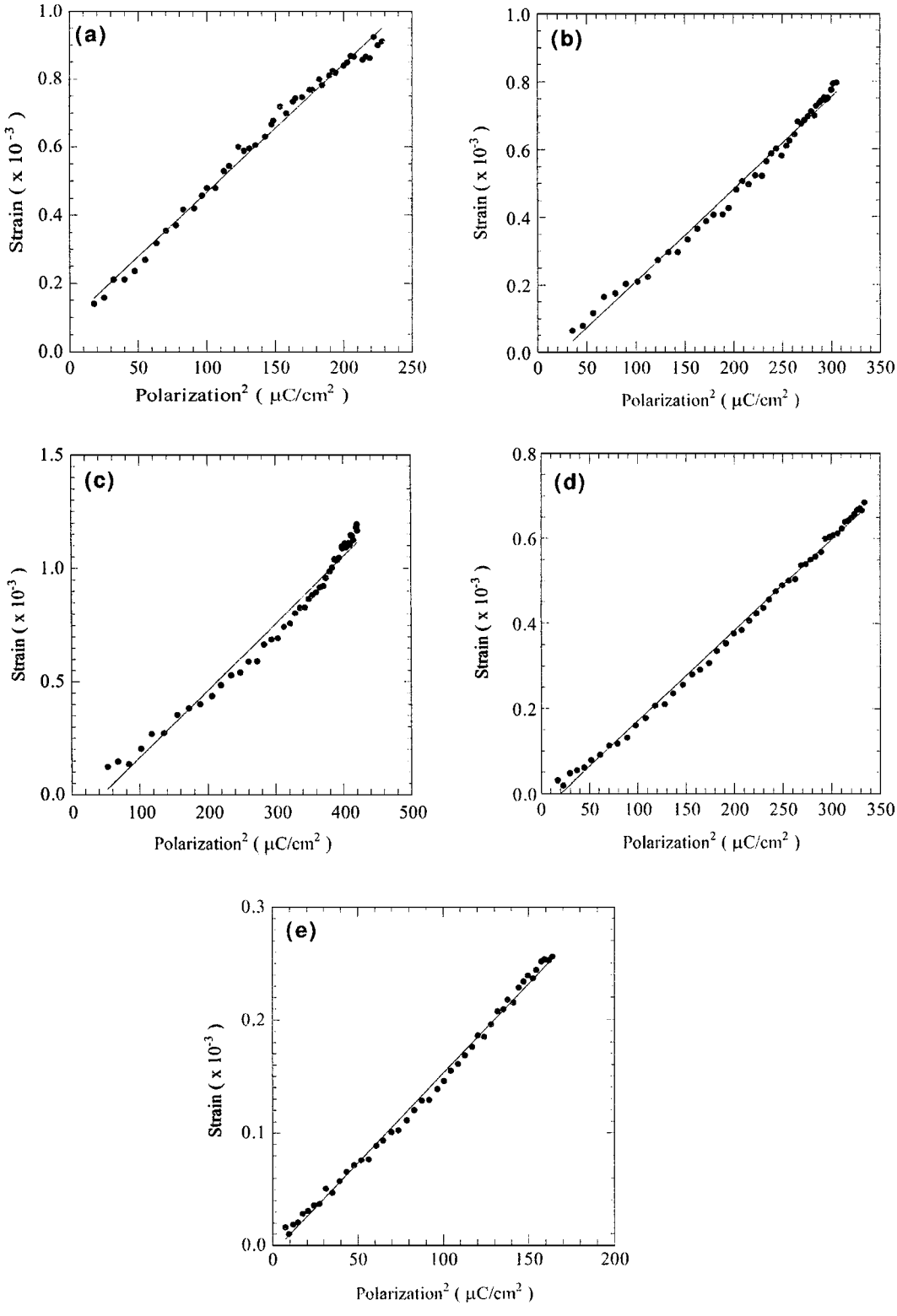

Figure 10 Electrically induced strain as a function of square of polarization in paraelectric region for (a) 0/65/35, (b) C-2/65/35, (c) C-5/65/35, (d) C-8/65/35 and (e) C-10/65/35.

where ε_{ij} is strain, P_k and P_l are polarization and Q_{ijkl} is electrostrictive coefficient. When ε_{ij} and P are parallel (or perpendicular) then the electrostrictive coefficient is the longitudinal Q_{11} (or transverse (Q_{12}). The electrostrictive coefficient can be calculated by measuring the slop of plot between ε and P^2.

Figs 9a–e and 10 a–e show plots of ε vs. P^2 (square of polarization) in the paraelectric region for compositions in the B-x/65/35 and C-x/65/35 sequences, respectively. A linear relation is evident between ε and P^2 in these figures. The electrostriction coefficient (Q_{11}) for different La-content samples in B-x/65/35 and C-x/65/35 are reported in Table II. These values are on the order of 10^{-2} consistent with earlier reported values [19]. It should be noticed from Table II that Q_{11} for C-x/65/35 is higher than for B-x/65/35 ($2 < x < 10$). This can be attributed to differences in the degree of non-stoichiometric ordering, as discussed in the previous section. The difference in the Q_{11} values are completely consistent with the empirical rule proposed for perovskite crystals [6].

TABLE II Electrostrictive coefficient comparison for B-x/65/35 and C-x/65/35 compositional sequences in paraelectric region

La-content (%)	Temperature (°C)	Q_{11} (B-x/65/35) (m^4C^{-2})	Q_{11} (C-x/65/35) (m^4C^{-2})
0	200	3.77×10^{-2}	—
2	160	3.30×10^{-2}	2.72×10^{-2}
5	80	2.83×10^{-2}	2.95×10^{-2}
8	25	1.60×10^{-2}	2.13×10^{-2}
10	25	2.23×10^{-2}	1.60×10^{-2}

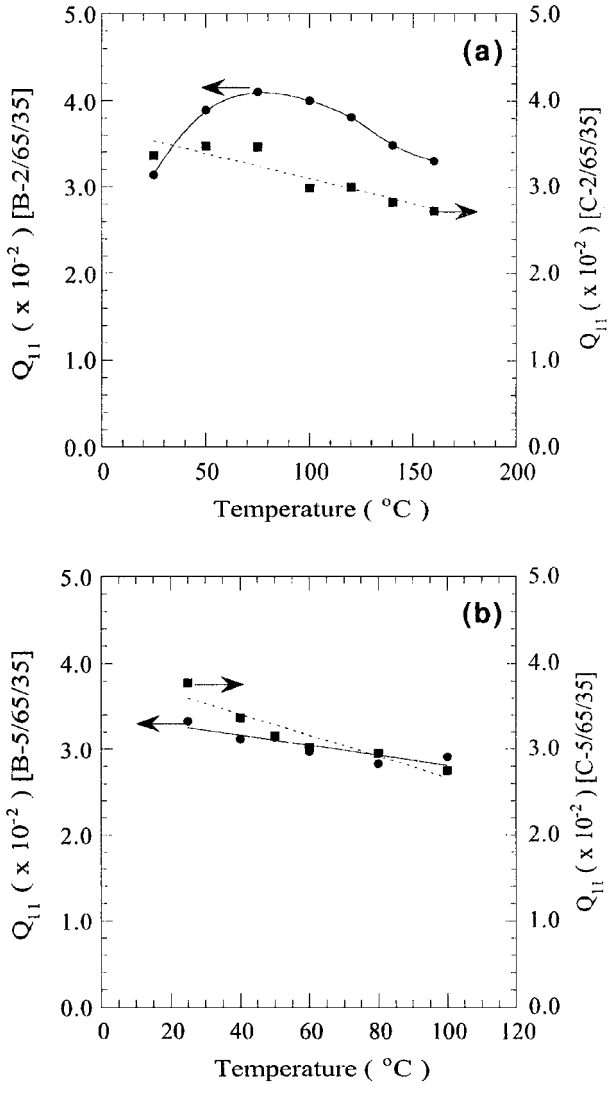

Figure 11 Comparison of electrostrictive coefficient (Q_{11}) as a function of temperature for (a) B-2/65/35 and C-2/65/35 and (b) B-5/65/35 and C-5/65/35.

The temperature dependence of Q_{11} for B&C-2/65/35 and B&C-5/65/35 are compared in Fig. 11a and b, respectively. It should be mentioned here that these samples showed "butterfly like" ε-E responses and are known to be ferroelectric near room temperature. In order to estimate a Q_{11} coefficient, ε and P were measured between 5 and 28 KV/cm electric fields. A linear relationship between ε and P^2 was found, and Q_{11} was estimated from the slope. Following this procedure, Q_{11} was found to first increase below 75 °C and then decrease above 75 °C for B-2/65/35 and to decrease for C-2/65/35 with increasing temperature. Similar decrease in Q_{11} with increase in temperature was found for B-5/65/35 and C-5/65/35 but later showed a larger temperature dependence than former. It seems Q_{11} is temperature independent only in paraelectric regions but it shows temperature dependence in ferroelectric regions, which can be attributed to domains.

4. Conclusions

Non-stoichiometric ordering in PMN-PT compositions close to the MPB showed pronounced effects on the electrostriction coefficient, and the electrically-induced strains and polarizations. A higher degree of non-stoichiometric ordering was found to yield a small induced polarization and larger strain. Selected area electron diffraction patterns are consistent with the electrostriction coefficient studies in which higher values of Q_{11} are related to stronger superlattice reflection intensity. Temperature dependent studies of the electrostriction coefficient revealed different trends for different charge compensation mechanisms. In order to achieve optimum strain for actuator applications, charge imbalance due to La^{3+} substitution on A-site should be compensated by changing B-site cation ratio.

Acknowledgements

This work was supported by the Office of Naval Research (ONR) under contract No. N00014-95-1-0805 and by Naval UnderSea Warfare Center contract No. N66604-95-C-1536. The use of the facilities in the Center for Microanalysis in Materials Research Laboratory at the University of Illinois at Urbana-Champaign is gratefully acknowledged. Helpful suggestions from our colleague Dr. Jie-Fang Li are gratefully acknowledged.

References

1. A. KUMADA, *Jpn. J. Appl. Phys.* **24**(24-2) (1985) 739.
2. K. UCHINO, Y. TSUCHIYA, S. NOMURA, T. SATO, H. ISHIKAWA and O. IKEDA, *Appl. Optics* **20** (1981) 3077.
3. M. GOMI, K. UCHINO, M. ABE and S. NOMURA, *Jpn. J. Appl. Phys.* **20** (1981) L-375.

4. S. NOMURA and K. UCHINO, *Ferroelectrics* **50** (1983) 197.
5. K. UCHINO, *Am. Ceram. Soc. Bull.* **65** (1986) 647.
6. K. UCHINO, S. NOMURA, L. E. CROSS, S. J. JANG and R. E. NEWNHAM, *J. Appl. Phys.* **51** (1980) 1142.
7. J. KUWATA, K. UCHINO and S. NOMURA, *Jpn. J. Appl. Phys.* **19** (1980) 2099.
8. S. NOMURA and K. UCHINO, *Ferroelectrics* **41** (1982) 117.
9. J. C. HO, K. S. LIU and I. N. LIN, *J. Mater. Sci.* **28** (1993) 4497.
10. D. VIEHLAND, M. C. KIM, J. F. LI and Z. XU, *Appl. Phys. Lett.* **67** (1995) 2471.
11. J. CHEN, H. M. CHAN and M. P. HARMER, *J. Amer. Ceram. Soc.* **72** (1989) 593.
12. C. A. RANDALL, D. J. BARBER, R. E. NEWNHAM and P. GROVES, *J. Mater. Sci.* **21** (1986) 4456.
13. N. DE MATHAN, E-HUSSON, P. GAUCHER and A. MORELL, *Mat. Res. Bull.* **25** (1990) 1427.
14. K. UCHINO, S. NOMURA, L. E. CROSS, R. E. NEWNHAM and S. J. JANG, *J. Mater. Sci.* **16** (1981) 569.
15. L. E. CROSS, S. J. JANG, R. E. NEWNHAM, S. NOMURA and K. UCHINO, *Ferroelectrics* **23** (1980) 187.
16. S. M. GUPTA and D. VIEHLAND, *J. Appl. Phys.* **80** (1996) 5875.
17. D. VIEHLAND and J. F. LI, *J. Appl. Phys.* **74** (1993) 4121.
18. A. G. KHACHATURYAN, *Phys. Rev. B* **48** (1993) 2949.
19. S. J. JANG, K. UCHINO, S. NOMURA and L. E. CROSS, *Ferroelectrics* **27** (1980) 31.

Received 21 May 1997
and accepted 9 April 1999